Journal of Applied Fluid Mechanics, Vol. 18, No. 1, pp. 159-170, 2025.
Available online at www.jafmonline.net, ISSN 1735-3572, EISSN 1735-3645.
https://doi.org/10.47176/jafm.18.1.2696

Numerical Study of Vertical Axis Wind Turbine with Spoiler Based on Orthogonal Experiments

Z. Hao, K. Chen †, T. Su, Z. Zhao and Q. Wang

School of Mechanical Engineering, Xinjiang University, Urumqi, China

†*Corresponding Author Email:* chenkun@xju.edu.cn

ABSTRACT

This paper investigated using spoilers to improve the aerodynamic characteristics of vertical-axis wind turbines. Taking the NACA0012 airfoil as the research object, the orthogonal experimental method design was employed to combine the parameters of the spoiler installation position. Then the wind energy utilization coefficient and the flow field structure of vertical-axis wind turbines were studied through numerical calculation, and the flow control mechanism of the spoiler and its effect on the aerodynamic performance of vertical-axis wind turbines were analyzed. The results show that the distance between the spoiler and the trailing edge of the blade is the main factor affecting the aerodynamic performance of vertical-axis wind turbines. By increasing the pressure difference between the suction and pressure surfaces of the blades, spoilers contribute to a higher aerodynamic performance of vertical-axis wind turbines. Additionally, the performance improvement effect on vertical-axis wind turbines is more significant at medium and low blade tip speed ratios. When the tip speed ratio is 1.8, the power coefficient of vertical axis wind turbines with spoilers is 25.3% higher than that of the original wind turbine.

Article History

Received March 4, 2024
Revised July 11, 2024
Accepted July 24, 2024
Available online November 6, 2024

Keywords:

Vertical axis wind turbine
Spoiler
Tip speed ratio
Passive flow control
Power coefficient

1. INTRODUCTION

The application of renewable energy has been a research hotspot in recent years, and wind energy, as an important component of renewable energy, has received much attention from various countries. The 2023 Global Wind Energy Report states that renewable energy generation is expected to account for 61% of total electricity generation by 2030 (GWEC, 2023). Improving the utilization of wind energy is currently a hot research direction.

At present, horizontal-axis wind turbines, as the mainstream of the wind power industry, have a large market share, but their blades have a complicated manufacturing process and high installation cost (Shah et al., 2018); vertical-axis wind turbines, on the other hand, because of their insensitivity to the wind direction, exhibit excellent performance in the environment of variable wind direction. Meanwhile, they have a low tower height, which reduces the installation cost, and their generators, gearboxes, and other major maintenance components are located on the ground, making the maintenance work more simpler and economical (Zhao et al., 2022). Since vertical-axis wind turbines may start at a slower wind speed, they can be employed to capture wind energy in areas with lower wind speeds, thereby extending the global reach of wind energy technology. Also, the relatively low noise levels make them particularly suitable for use in urban and residential environments (Wong et al., 2018). Therefore, it is gradually gaining importance.

The problems faced by vertical-axis wind turbines in the development process mainly include their relatively low energy efficiency, difficulty in self-starting under low wind speed conditions, and challenges in structural stress and durability. (Chehouri et al., 2015). These problems limit their potential in large-scale power generation applications, thus affecting the overall economic feasibility, technological innovation and cost reduction. However, through technological innovation, optimized design, as well as advances in materials, it is expected to solve these problems and improve the energy efficiency and reliability of vertical axis wind turbines.

To enhance the vertical-axis wind turbines' aerodynamic performance, scholars at home and abroad have conducted much research on various flow control techniques.

Bianchini et al. (2019) have shown that using Gurney flaps leads to a significant improvement in the aerodynamic performance of the blade, with a 58% increase in the peak lift coefficient over the baseline configuration. Meanwhile, the whole lift curve is greatly

NOMENCLATURE

c	airfoil chord length	*U*	inlet wind speed
Cp	power coefficient	λ	Tip Speed Ratio (TSR)
H	spanwise length	θ	Azimuthal angle
D	rotor diameter	*R*	rotor radius

shifted upward without large changes in drag coefficient, and the aerodynamic performance can be substantially improved by choosing a suitable Gurney flap configuration at low to medium tip speed ratios.

Zhu et al. (2022a) investigated the application of bionic blades in vertical axis wind turbines, the average increases in the power coefficient of bionic blades with the increase in TSR, and it was found that the high wind energy utilization in the wave trough section is the main reason why bionic blades are better than standard blades.

Li et al. (2023) studied the use of wind collectors in vertical-axis wind turbines with straight blades. The wind collector was installed on the upper and lower sides of the rotor. It was found that the installation of the wind collector can increase the wind area of the wind turbine increase and improve the aerodynamic performance of vertical-axis wind turbines at low wind speeds.

Ahmadi-Baloutaki et al. (2016) investigated the performance of several vertical-axis wind turbines arranged in different formations in a wind tunnel, and they analyzed the interaction of the wind turbines in the arrangement. It was found that the reverse rotation of the wind turbines in the array slightly improves the aerodynamic performance compared to a single vertical-axis wind turbine; meanwhile, the co-rotation slightly reduces the aerodynamic performance in some cases.

Spoilers, as a common aerodynamic component, are widely used in automobiles (Chen et al. 2022), airplanes (Hu & Fu, 2023), ships (Hou et al., 2023), and other mechanical structures. Their main function is to change the characteristics of the fluid to improve stability, reduce drag, or control lift.

The application of spoilers can improve the flow field structure and improve its aerodynamic performance, but the above research is mostly applied to equipment such as automobiles, ships, aircraft, and horizontal-axis wind turbines(Ge et al., 2022), with less research on vertical-axis wind turbines. Therefore, this paper investigates the possibility of installing spoilers on the blades of vertical-axis wind turbines and analyzes the impact of spoilers at different positions on aerodynamic performance. Additionally, the optimal spoiler position parameters are obtained to further improve the aerodynamic characteristics of vertical-axis wind turbines.

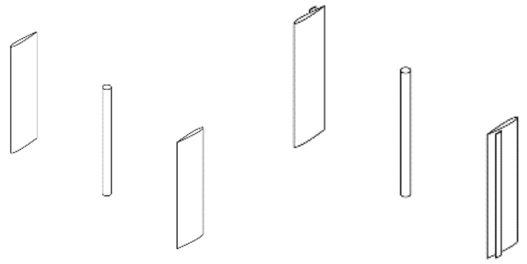
(a) (b)

Fig. 1 The simplified 3D model of the vertical-axis wind turbine (a) and vertical axis wind turbine with a spoiler (b)

2. COMPUTATIONAL MODELLING AND MESHING:

2.1 Computational Models

In this paper, a spoiler is added at the trailing edge of the blade to modify the blade. Figure 1 (a) shows the prototype of the vertical-axis wind turbine, and Fig.1 (b) shows the prototype of the vertical-axis wind turbine with a spoiler. The connection between the rotor shaft and the blades is neglected.

Figure 2 (a) is a schematic diagram of the blade with a spoiler, where c denotes the chord length of the blade. Figure 2 (b) is a schematic diagram of the installation parameters of the spoiler. Four specific parameters are used to determine the position of the spoiler, including the distance from the center of the spoiler to the trailing edge of the blade, the chord length of the spoiler, the distance from the center of the spoiler to the surface of the blade, and the angle of rotation of the spoiler relative to the blade. In Fig. 2 (b), A denotes the distance between the center of

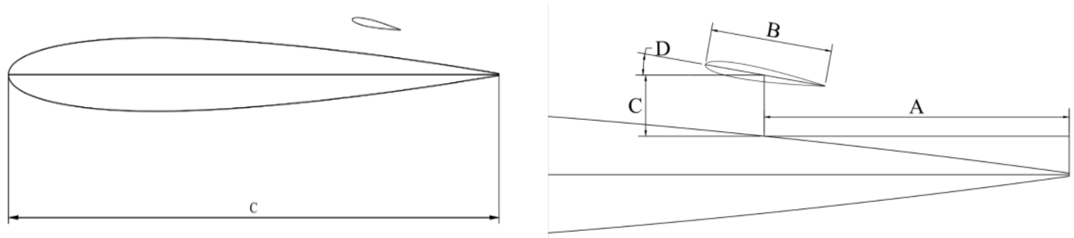

（a） (b)

Fig. 2 Schematic diagram of spoiler blade and its localization

the spoiler and the trailing edge of the blade. B denotes the chord length of the spoiler, C denotes the vertical distance between the center of the spoiler and the surface of the blade, and D denotes the angle at which the spoiler rotates relative to the blades. These four parameters determine the position and size of the spoiler relative to the blades, and the optimal relative position and size of the spoiler can be determined by adjusting the values of these four parameters.

The vertical axis wind turbine in the literature (Subramanian et al., 2017) is taken as the research object of this paper, the symmetric profile type NACA0012 is selected, and the specific parameters are listed in Table 1.

The spoiler airfoil type is NACA0012 as that of the prototype blade. In Fig. 3, the inlet wind speed (U) is 10 m/s, θ denotes the blade phase angle, ω denotes the angular velocity and R denotes the rotor radius. The key performance indicators of the wind turbine mainly include the moment coefficient (Cm), the power coefficient (Cp), and the blade tip velocity ratio (λ).

$$C_m = \frac{M}{\frac{1}{2}\rho c U_\infty^2 [2RH]} \quad (1)$$

$$C_p = \frac{P}{\frac{1}{2}\rho U_\infty^3 [2RH]} \quad (2)$$

$$TSR = \frac{\omega R}{U} \quad (3)$$

Where, M denotes the average torque(N/m), ρ denotes the horizontal incoming air density(kg/m^3), P denotes the output power (Watt).

2.2 Computational Structure and Meshing

The computational domain is a rectangular prism with a length of 15 D, a width of 10 D, and a height of 1.8 m, where D is the rotor diameter. The cylindrical area with a diameter of 1.5 D in the computational domain is the rotation domain, as shown in Fig. 4 (a) (Zhu et al., 2022b). The blades of the vertical-axis wind turbine studied in this paper have geometrically symmetric shapes, so only the upper part of the wind turbine is modeled. Figure 4 (b) shows the overall mesh division, with the middle rotation domain encrypted. Figure 4 (c) shows the grid division around the blade. Select the tetrahedral grid. The thickness of the first layer of the boundary layer is 0.06 mm, leading to an average y+ value around 1. The average grid mass is greater than 0.75, the maximum skewness is less than 0.9, the Reynolds number is 2.875×10-5, the inlet wind speed is set to 10 m/s, and the pressure at the outlet is 1 atm. Figure 4 (d) shows the grid around the blade with a spoiler.

Table 1 Main parameters

Parameters	Values	Parameters	Values
blade number	2	chord length	0.420 m
airfoil	NACA0012	rotor diameter	2.7 m
incoming flow rate	10 m/s	Blade height	3 m
tip speed ratio	1-3	angular velocity	7.4-22.22 rad/s

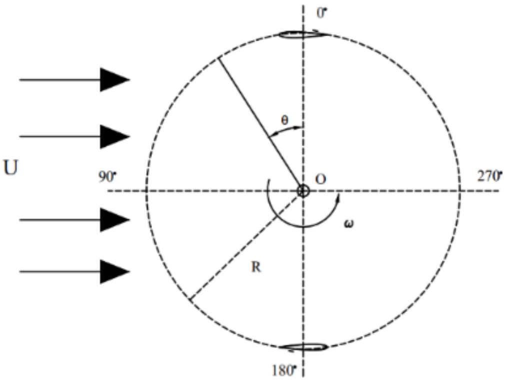

Fig. 3 Vertical-axis wind turbine with spoilers

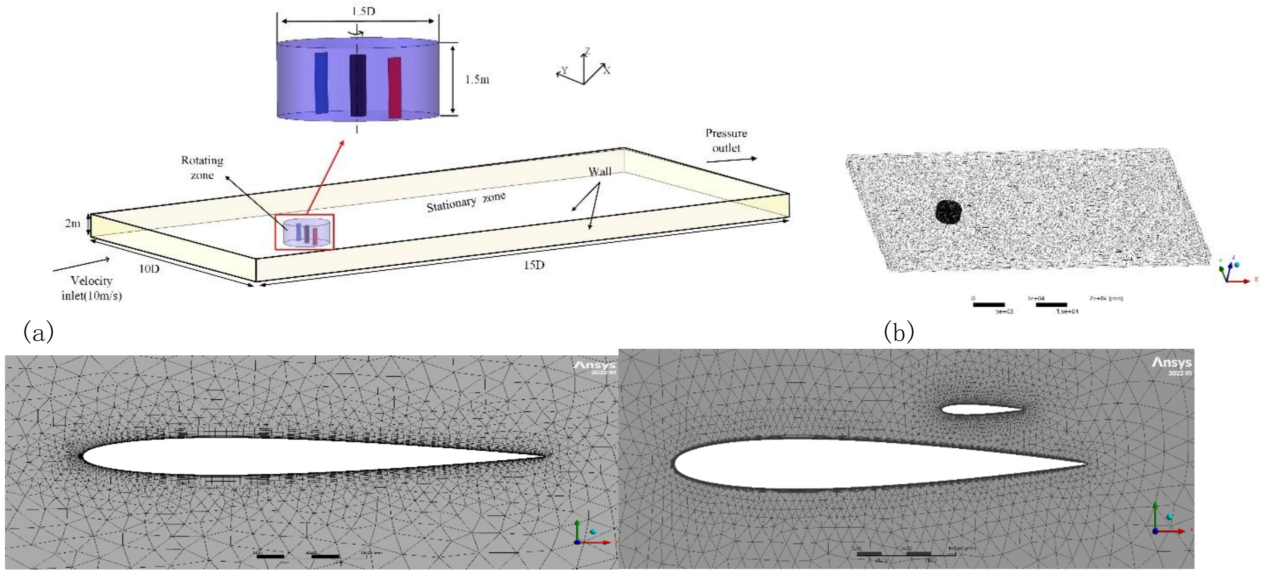

Fig. 4 Flow field and meshing in the computational domain

3. CALCULATION METHOD

In this paper, the SIMPLEC algorithm is utilized to perform numerical simulation by using Ansys Fluent computational fluid dynamics software. Compared with other turbulence models, the SST k-ω turbulence model can better match the experimental values of vortex volume, wind energy utilization factor, as well as wake and velocity distributions at the optimal blade tip speed ratio when simulating the dynamic stall of a vertical axis wind turbine (Rezaeiha et al., 2018). Therefore, this turbulence model is selected for solution in this paper. Studies have shown that the time step size in the CFD simulation of vertical axis wind turbines has a small impact on the accuracy (Zhu et al., 2022b). Based on this, in this paper, the time step is the time corresponding to a rotation angle of 1° of the wind turbine blades, and the stability results of the 10th cycle are taken for analysis.

The governing equations for CFD simulations are the non-stationary Reynolds averaged Navier Stokes (URANS) equations, which are expressed as:

$$\frac{\partial \rho U}{\partial t} + \nabla \cdot (\rho U U) = -\nabla \left(P + \frac{2}{3}\mu \nabla \cdot U\right) + \nabla \cdot [\mu(\nabla U + (\nabla U)^T)] \quad (4)$$

Where r denotes the density, μ denotes the viscosity, and U denotes the velocity. The momentum equation can be simplified as follows:

$$\frac{\partial U}{\partial t} + \nabla \cdot (UU) = -\nabla p + \nabla \cdot \left(v_{eff} \nabla U\right) \quad (5)$$

Where p denotes the dynamic pressure, and v_{eff} denotes the effective kinematic viscosity.

The continuity equation can be simplified as follows:

$$\frac{\partial \rho}{\partial t} + \nabla \cdot (\rho \mathbf{v}) = 0 \quad (6)$$

Where ρ denotes the fluid density, and $\mathbf{v}$ denotes the velocity vector of the fluid.

3.1 Validation of the Number of Grids

This study simulates the mesh division of 2.06 million, 5.60 million, and 9.63 million at a tip speed ratio of 1.5. The calculation results are shown in Fig. 5. The x-axis represents the phase angle (θ), and the y-axis represents the torque coefficient (C_m). A great change can be observed in the instantaneous torque coefficient compared to the number of grids in the computational domain of 2.06 million and 5.60 million. The wind energy utilization coefficient is 0.34 for a 2.06 million grid, and 0.23 for a 5.60 million grid. The instantaneous torque coefficients of 5.60 million and 9.63 million grids basically overlap, and the wind energy utilization coefficient of 9.60 million grid is 0.22, with a difference of less than 5% compared to that of the 5.60 million grids. The 5.60 million grids can meet the simulation requirements, so is selected as the basic grid for numerical calculation.

3.2 Comparative Experimental Validation

This paper conducted a study using a commercially feasible 1.1 kW Darrieus VAWT, and the results compared

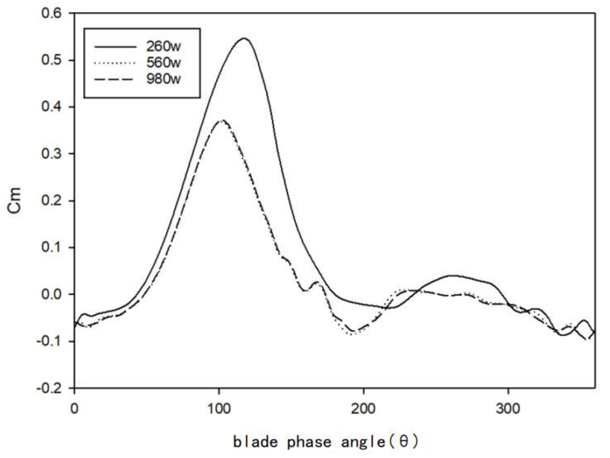

Fig. 5 Comparison of instantaneous moment coefficients for three quantities of meshes

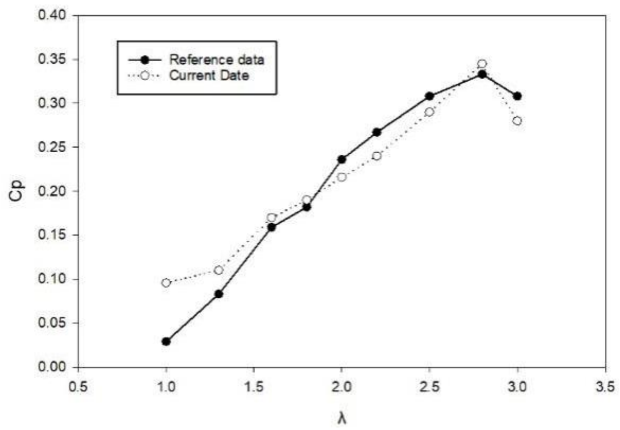

Fig. 6 Comparison of wind energy utilization factor between simulation and experimental results.

to reference date (Subramanian et al., 2017) are shown in Fig. 6. When removing λ within the range of 1, the average deviation is 10.07%. When removing λ at a tip speed ratio of 1, the simulation and experiment have good similarity, and the calculation error is small, and falls within an acceptable range, indicating that the calculation results have high accuracy and reliability.

3.3 Orthogonal Experimental Design

The relative position between the spoiler and the blade can be determined based on the four parameters mentioned in the previous section. Conducting comprehensive experiments requires a huge amount of calculation, so the orthogonal experiment method is employed to analyze the influence of various factors, and obtain the optimal combination method. The above four parameters are taken as the four factors of the orthogonal experimental design, and the size relative to the blade is taken as the horizontal parameter. Then, orthogonal experiments are designed based on this.

The four factors of the orthogonal experiment are the distance between the center of the spoiler and the trailing edge of the blade (A), the chord length of the spoiler (B), the vertical distance between the center of the spoiler and

Table 2 Factors of orthogonal experimental design

Items		Factors			
		A	B	C	D
Levels	1	0.25c	0.1c	0.05c	-10°
	2	0.5c	0.2c	0.1c	0°
	3	0.75c	0.3c	0.15c	10°

Table 3 Results of orthogonal experiments

Items	Levels				Cp
	A	B	C	D	
1	105	42	21	-10	0.204
2	105	84	42	0	0.228
3	105	126	63	10	0.171
4	210	42	42	10	0.186
5	210	84	63	-10	0.165
6	210	126	21	0	0.129
7	315	42	63	0	0.126
8	315	84	21	10	0.124
9	315	126	42	-10	0.05

the surface of the blade (C), and the rotation angle of the spoiler relative to the blade (D). The selection of horizontal factors is relative to the chord length of the blade, and the relative rotation angle. The distance between the spoiler and the trailing edge of the blade is selected as 0.25c, 0.5c, and 0.75c. The chord length of the spoiler is selected as 0.1c, 0.2c, and 0.3c. The distance between the spoiler and the blades is selected as 0.05c, 0.1c, and 0.15c. Additionally, the rotation angle is selected as -10 °, 0 °, and 10 °.

4. RESULTS AND ANALYSIS

4.1 Orthogonal Experiment Polar Analysis

The orthogonal test was conducted at a leaf tip speed ratio of 1.8, taking the power coefficient Cp as an evaluation indicator, and the effects of the factors were analyzed through nine simulations. The simulation results are presented in Table 3. From this table, it can be seen that the power coefficient of the vertical-axis wind turbine with spoilers is significantly increased compared to the prototype wind turbine for the combination of some spoiler mounting positions.

To analyze the improvement of some combinations in Table 3 for the overall power factor of the vertical axis wind turbine, the data in Table 3 are analyzed in terms of mean and extreme deviation, as listed in Table 4. Here, K1, K2, K3, and K4 represent the sum indicators of factors A, B, C, and D, while k1, k2, k3, and k4 are the arithmetic means corresponding to factors A, B, C, and D. R denotes the extreme deviation of each of the factors A, B, C, and D, and it measures the range of changes in the indicators at different levels.

For the orthogonal experimental method, the larger the range of changes, the higher the degree of influence of the corresponding factors on the indicators; The larger the arithmetic mean, the better the corresponding factor. The

Table 4 Arithmetic mean and range

Items	Levels			
	A	B	C	D
K1	0.6030	0.5160	0.4570	0.4190
K2	0.4800	0.5173	0.4643	0.4830
K3	0.300	0.3500	0.4620	0.4810
k1	0.2011	0.1720	0.1523	0.1397
k2	0.1600	0.1724	0.1547	0.1611
k3	0.100	0.1166	0.1540	0.1603
R	0.101	0.0558	0.0024	0.0214

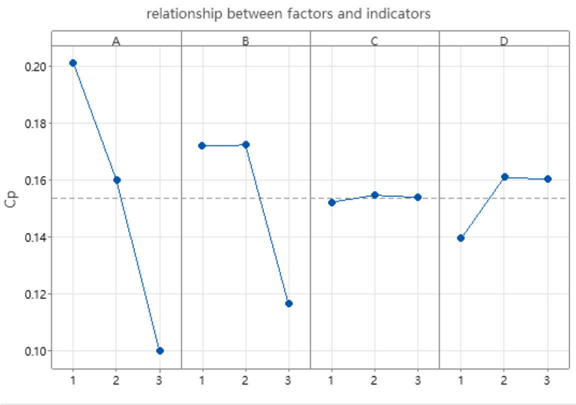

Fig. 7 Relationship between factors and indicators

optimal combination can be obtained by using Cp as the vertical axis and each k value as the horizontal axis. According to the size of the data in row R, factor A has the largest difference and the greater influence on the indicator, factor B has the second-highest degree of influence, factor D has the third-highest degree of influence, and factor C has the lowest degree of influence. According to the data in Fig. 7, it can be concluded that k1 reaches the maximum value in column A, k2 reaches the maximum value in column B, k2 reaches the maximum value in column C, and k2 reaches the maximum value in column D. Therefore, A1B2C2D2 is the optimal design solution, and its power coefficient reaches 0.228, showing an improvement of 25.3% compared with the original vertical-axis wind turbine.

4.2 Analysis of the Mechanism of Better Spoiler Action

In this study, the power coefficients of vertical-axis wind turbines with spoilers are compared with those of the original vertical-axis wind turbines at different tip-speed ratios. The relevant results are illustrated in Fig. 8, and the optimal combination is selected as the specific installation position of the spoiler through the optimization of the orthogonal test.

From Fig. 8, it can be seen that the power coefficient of the vertical-axis wind turbine equipped with spoilers is significantly larger at low and medium blade tip speed ratios. The power coefficient of the wind turbine with spoilers is much higher than that of the original design at tip ratios between 1.3 and 2.5, while it is slightly lower than that of the original design at a tip ratio of 1. In particular, the wind energy utilization factor reaches a

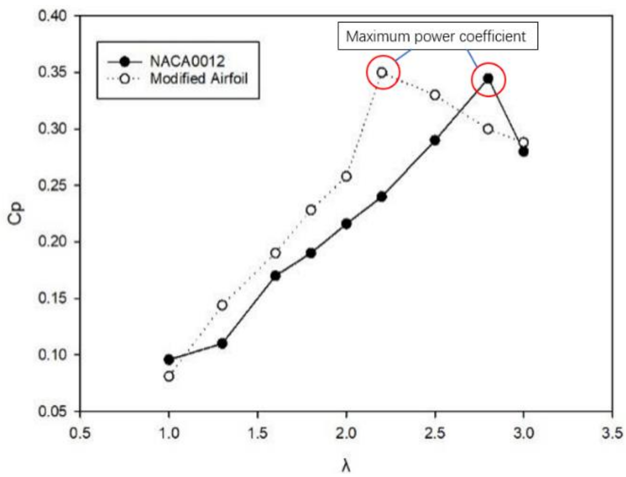

Fig. 8 Variation of average wind energy utilization factor（Cp）with leaf tip speed ratio (λ)

maximum value of 0.35 when the tip speed ratio reaches 2.2. Additionally, the wind energy utilization factor shows a continuous increasing trend when the tip speed ratio increases from 1 to 2.2, but it decreases rapidly when the tip speed ratio exceeds 2.2. In contrast, the wind energy utilization factor of the original design peaks at a tip speed ratio of 2.8, and then it gradually decreases as the tip speed ratio is further increased. At a tip speed ratio of 1, the power coefficient of the modified airfoil decreased by 15% compared to the NACA0012 airfoil. At the tip speed ratios of 1.3, 1.5, 1.8, 2, and 2.5, the power coefficient of the modified airfoil increased by 30%, 11%, 20%, 19%, 45%, and 10%, respectively. At a tip speed ratio of 2.8, the modified airfoil power coefficient decreased by 10%. At a tip speed ratio of 3, the modified airfoil power coefficient increased by 2%. Overall, the installation of spoilers improves the aerodynamic performance of blades at most blade tip speed ratios.

Figure 9 shows the instantaneous torque comparison between a vertical axis wind turbine with a spoiler and a prototype wind turbine at a blade tip speed ratio of 1.8. In the phase angle range of [80 °, 180 °], the spoiler can effectively enhance the aerodynamic performance of vertical axis wind turbines, leading to a significant increase in instantaneous torque. In the phase angle range of [0 °, 80 °], the instantaneous torque of the vertical-axis wind turbine with a spoiler is slightly lower than that of the prototype vertical-axis wind turbine without a spoiler. When the phase angle reaches 120 °, the vertical-axis wind turbine with a spoiler reaches its maximum instantaneous torque coefficient. Meanwhile the installation of the spoiler significantly improves the aerodynamic efficiency of the blades and increases the instantaneous torque of the vertical axis wind turbine. When the phase angle exceeds 120 °, the instantaneous torque coefficient gradually decreases. When the phase angle exceeds 160 °, the instantaneous torque coefficient remains the same as the original airfoil. Within the phase angle of [160 °, 240 °], the vertical-axis wind turbine with a spoiler has a slightly lower instantaneous torque coefficient than the prototype wind turbine. Within the phase angle of [240 °, 360 °], the instantaneous torque coefficients of the two are almost the same.

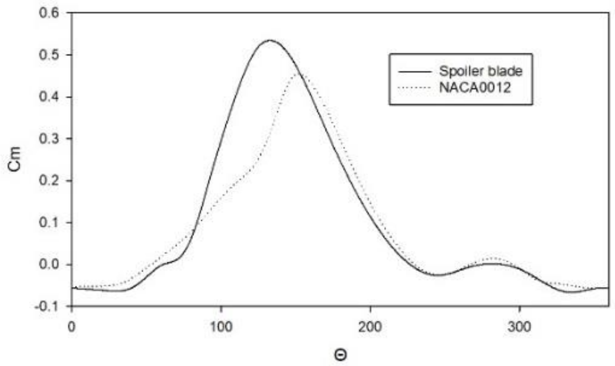

Fig. 9 variation of blade torque with phase angle at λ=1.8

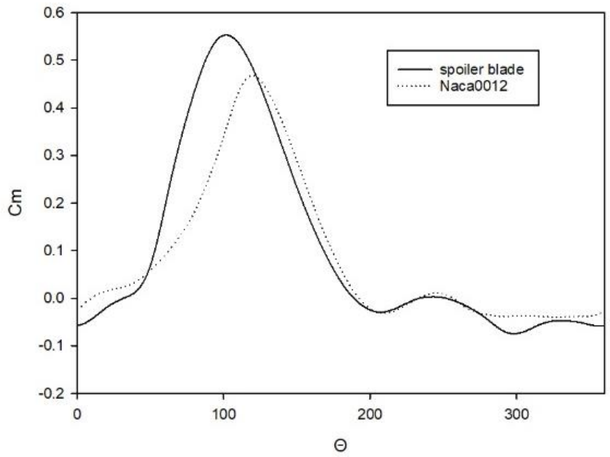

Fig. 10 variation of blade torque with phase angle at λ=2

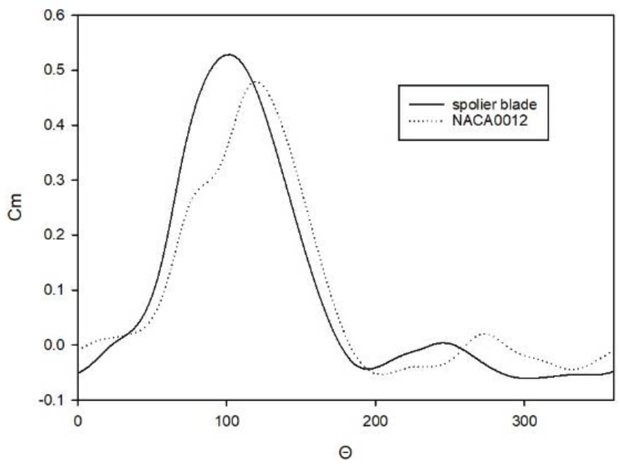

Fig. 11 variation of blade torque with phase angle at λ=2.5

Figure 10 shows the comparison of the instantaneous torque between a vertical-axis wind turbine with a spoiler and a prototype wind turbine at a tip speed ratio of 2. Within the phase angle range of [50 °, 120 °], the spoiler can effectively enhance the aerodynamic performance of the vertical-axis wind turbine, resulting in a significant increase in its instantaneous torque. Within the phase

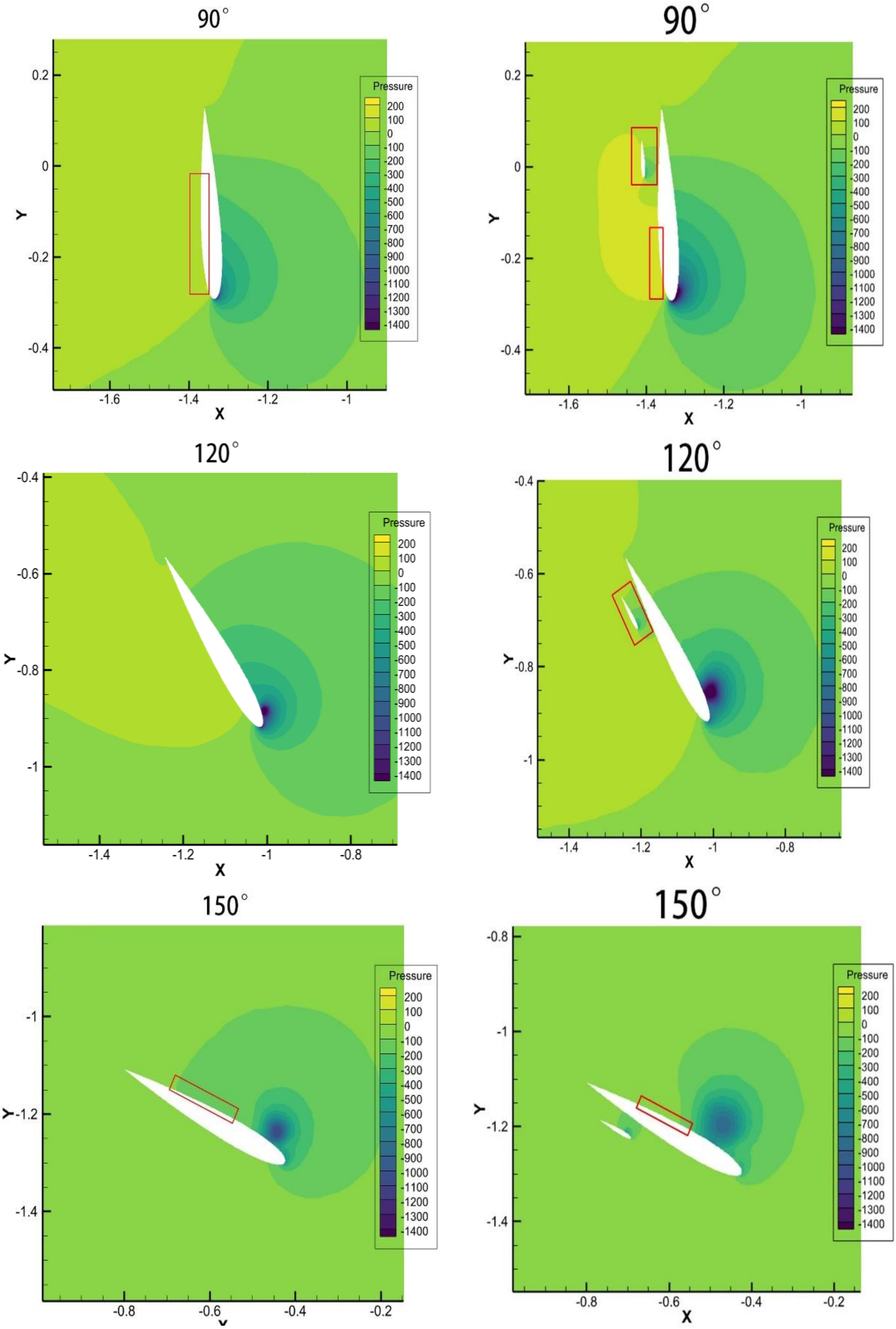
90°
90°
120°
120°
150°
150°
Pressure
200
100
0
-100
-200
-300
-400
-500
-600
-700
-800
-900
-1000
-1100
-1200
-1300
-1400
X
Y

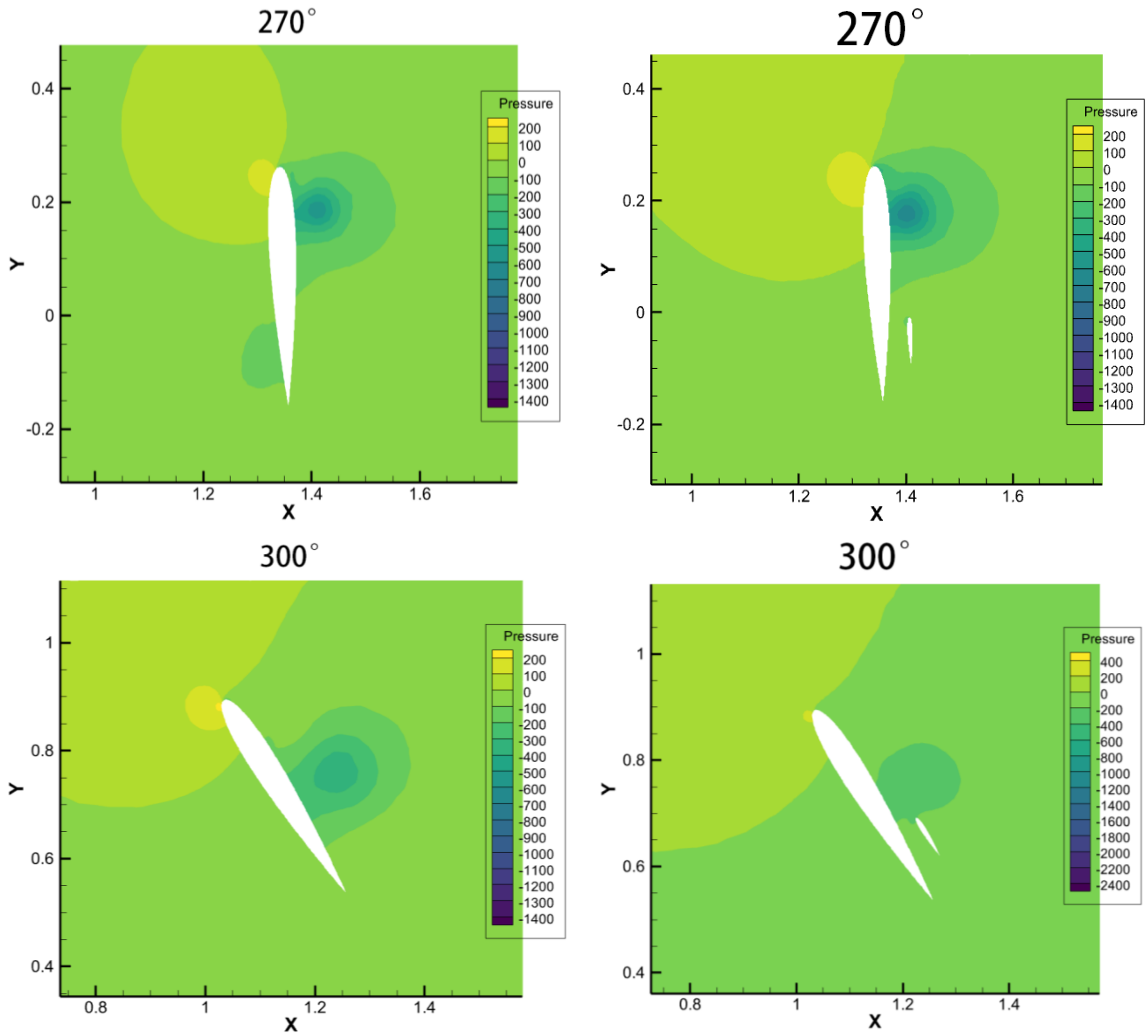

(a) (b)

Fig. 12 Pressure contours, (a) listed as prototype blade, (b) listed as blade with spoilers

angle range of [0 °, 50 °], the instantaneous torque of the vertical axis wind turbine with a spoiler is slightly lower than that of the prototype vertical axis wind turbine without a spoiler. When the phase angle reaches 100 °, the vertical-axis wind turbine with a spoiler reaches its maximum instantaneous torque coefficient. When the phase angle exceeds 100 °, the instantaneous torque coefficient gradually decreases. When the phase angle exceeds 130 °, the instantaneous torque coefficient remains the same as the original airfoil. Within the phase angle range of [130 °, 280 °], the instantaneous torque coefficients of the two are almost the same. Within the phase angle range of [280 °, 360 °], the vertical-axis wind turbine with a spoiler is slightly lower than that of the prototype wind turbine.

Figure 11 shows the comparison of instantaneous torque between a vertical-axis wind turbine with a spoiler and a prototype wind turbine at a tip speed ratio of 2.5. Within the phase angle range of [50 °, 120 °], the spoiler can effectively increase the aerodynamic performance of the vertical-axis wind turbine. Within the phase angle range of [0 °, 50 °], the instantaneous torque of the vertical-axis wind turbine with a spoiler is slightly lower than that of the prototype vertical-axis wind turbine without a spoiler. When the phase angle reaches 110 °, the vertical-axis wind turbine with a spoiler reaches its maximum instantaneous torque coefficient. When the phase angle exceeds 110 °, the instantaneous torque coefficient gradually decreases. Within the phase angle range of [120 °, 190 °], the vertical-axis wind turbine with a spoiler has a slightly lower instantaneous torque coefficient than the prototype wind turbine.

Overall, the addition of spoilers increases the torque coefficient of the blades in the upwind region, while the impact on the torque coefficient is relatively small in the downwind region.

Figure 12 shows the pressure contours around the prototype blade and the blade with a spoiler installed at partial phase angles. Specifically, Fig. 9(a) shows the pressure contour map of the prototype blade, while Fig. 9(b) shows the pressure contour map of the blade with a

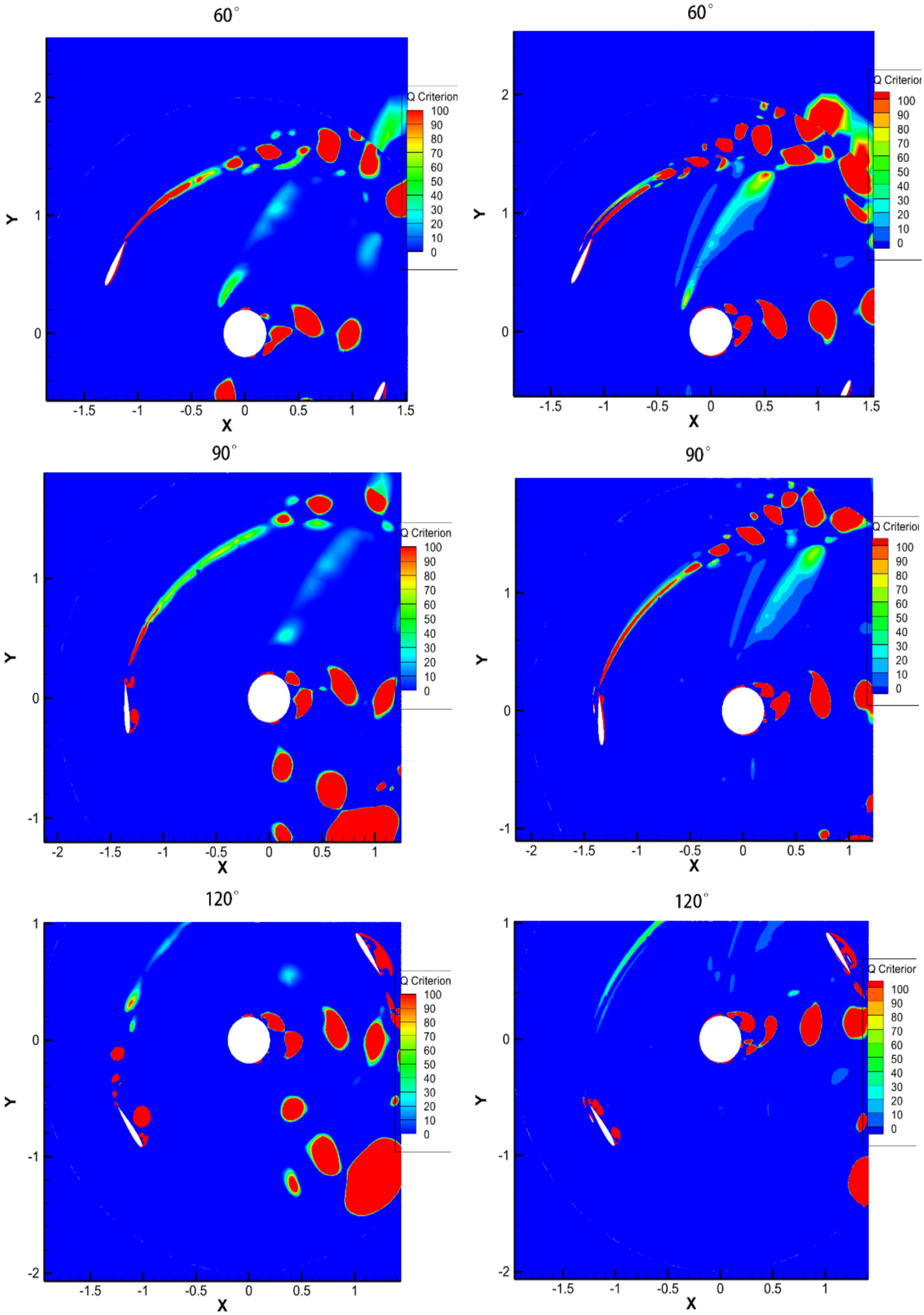
60°
60°
90°
90°
120°
120°
Q Criterion
100
90
80
70
60
50
40
30
20
10
0
X
Y
-2
-1.5
-1
-0.5
0
0.5
1
1.5
2

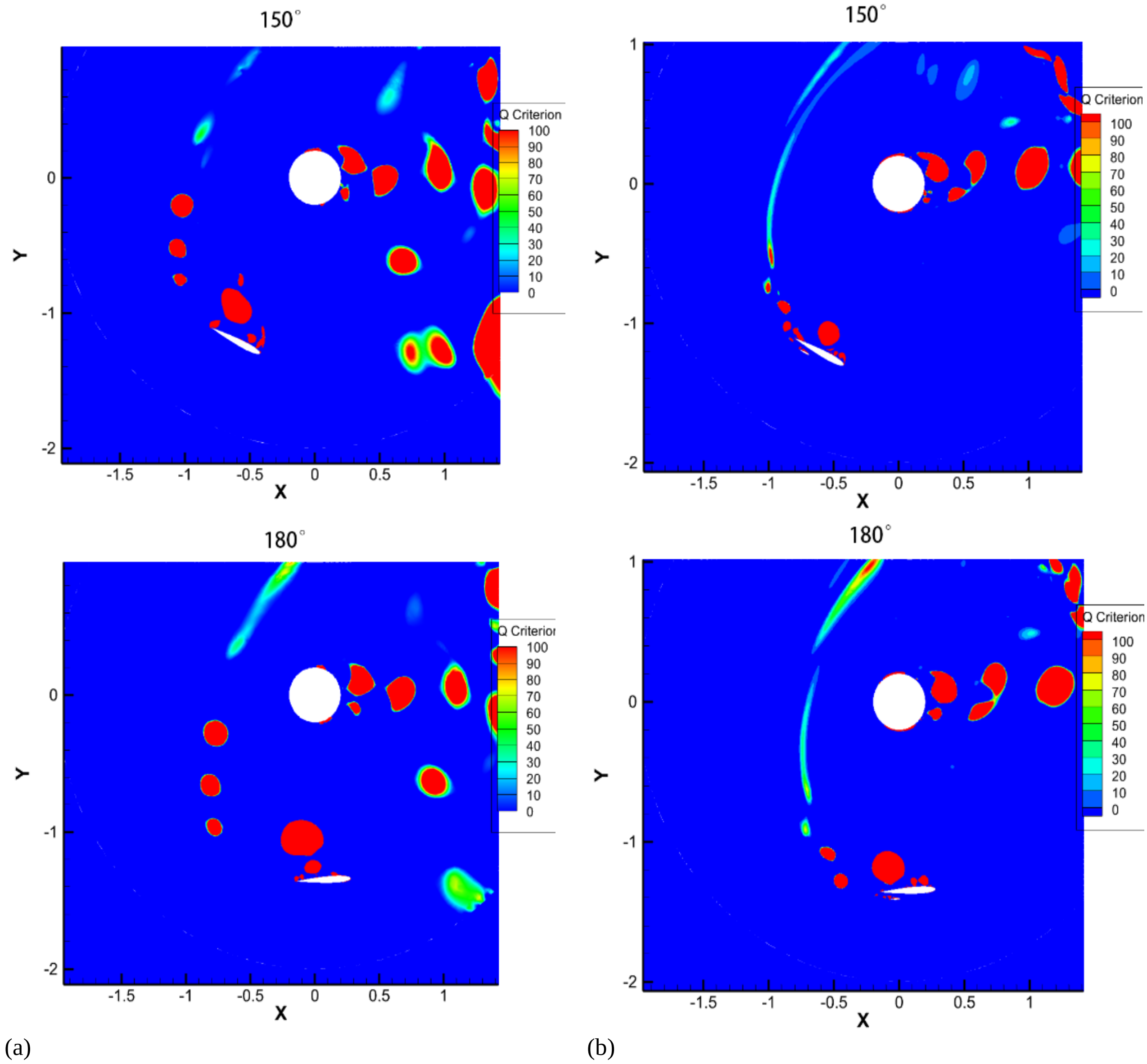

Fig. 13 Vortex cloud, (a) column for the prototype blade, (b) column for the blade with spoilers

spoiler. At a phase angle of 90 °, the pressure on the pressure surface of the blade with a spoiler is significantly higher than that of the prototype blade, and the pressure on the suction surface is slightly lower than that of the prototype blade. Also, there is a large pressure difference on both sides of the spoiler, and the overall pressure difference of the blades with a spoiler is significantly greater than that of the prototype blade. Meanwhile, the torque coefficient of the modified blades is significantly increased compared to that of the prototype blade. When the phase angle reaches 120 °, the pressure range on the pressure surface of the blade with a spoiler increases compared to that of the prototype blade, but the change in pressure magnitude is not significant. Compared with the prototype blade, the blade with a spoiler does not exhibit any changes in the low-pressure area of the suction surface, but the magnitude of pressure is reduced. Also, there is a certain pressure difference on both sides of the spoiler. Overall, the installation of the spoiler increases the pressure difference on both sides of the blade and enhances the instantaneous torque. When the phase angle is 150 °, the difference between the pressure on the pressure surface and the pressure on the suction surface of the blade with a spoiler and the prototype blade is very small. However, the presence of a spoiler increases the range of low-pressure areas on the suction surface of the blade, and there is a pressure difference on both sides of the spoiler. Overall, the pressure difference of the blade with a spoiler is larger than that of the prototype blade, but the difference is limited. When the phase angle is 270 °, the blade with a spoiler has little change in pressure and suction surfaces compared to the prototype blade. The installation of the spoiler has little effect on the torque coefficient of the blades. When the phase angle is 300 °, the installation of the spoiler hardly affects the pressure and pressure difference of the blade pressure surface and suction surface, without changing the torque coefficient of the blade. The installation of the spoiler increases the torque coefficient of the blade during the upstream stroke, and it has a smaller impact on the blades during the downstream stroke.

Figure 13 shows a comparison of the vortex maps of the prototype blade and the blade with a spoiler at different phase angles. The simulation was conducted without neglecting the axis, which generates wake in a smooth flow. Since all the results were obtained under the same axis size, it has a relatively small impact on the comparison of the two different blades. In the phase angle range of [60°, 90°], the wake vortices produced by the modified and prototype wind turbines are almost the same in terms of number and location, indicating that the addition of a spoiler does not improve the overall aerodynamic performance of the wind turbine. At a phase angle of 120°, the prototype blade begins to form a few small shedding vortices in the direction of travel, while the blade with a spoiler produces almost no shedding vortices. This suggests that at this phase angle, the prototype wind turbine blade shows more significant flow separation, a phenomenon that affects aerodynamic performance. In the phase angle range of [120°, 150°], shedding vortices start to appear at the trailing edge of the blade with a spoiler, but the number is significantly smaller than that of the prototype blade. The addition of spoilers hinders vortex formation in the upwind region and reduces the number of shedding vortices, leading to a more stable flow field and higher aerodynamic efficiency of the wind turbine. The wake generated by the spoiler is added to the wake of the main blades, leading to more serious downstream wake deficiency. This affects the performance of the blades in the downwind area and potentially affects the rear wind turbines in a wind turbine array.

5. Conclusion

1) To solve the problem of low power coefficient of vertical-axis wind turbines, this paper proposes a design scheme of adding spoilers to the blades. The vertical-axis wind turbine equipped with spoilers is analyzed by three-dimensional aerodynamic simulation and optimized by using the orthogonal test method. The results indicate that among the four factors considered in this paper, the installation distance of the spoiler relative to the trailing edge of the blade is the most important, which has the largest influence on the aerodynamic performance of the wind turbine, while the influence of the installation angle of the spoiler is relatively small.

2) The installation of spoilers with a tip speed ratio between 1.3 and 2.3 can effectively increase the power factor of vertical-axis wind turbines. For instance, at a tip speed ratio of 1.8, the optimized spoiler configuration increases the average wind energy utilization of the wind turbine by 25.3% compared to the original un-optimized design. The installation of the spoiler has a regulatory effect on the flow field around the blade, i.e., increasing the pressure difference between the two sides of the blade; the spoiler also exhibits a pressure difference between its two sides at some phase angles, which improves the overall aerodynamic performance of the wind turbine. This design improvement provides an effective method for improving the performance of vertical-axis wind turbines.

3) The installation of the spoiler effectively suppresses the flow separation on the blade surface at a certain phase angle, and the wake generated by the spoiler is added to the wake of the main blade. This may lead to more insufficient wake downstream, affecting the performance of the blades in the downwind area and affecting the rear row wind turbines in wind turbine arrays.

4) The power coefficient of vertical-axis wind turbines equipped with spoilers starts to decrease gradually when the blade tip speed ratio exceeds 2.3. However, the spoiler performs well at low and medium blade tip speed ratios, which is a new research direction to consider.

Acknowledgements

This study was funded by the National Natural Science Foundation of China (No.5220053067); the Natural Science Foundation of Xinjiang Uygur Autonomous Region, China (No.2022D01C33);

Conflict of Interest

The authors declare that they have no known competing financial interests or personal relationships that might influence the work reported here.

Authors Contribution

Zhenhua Hao: Data curation, Writing – original draft, Conceptualization, Investigation, Methodology, Software, Formal analysis; **Kun Chen:** Writing – review & editing, Project administration, Funding acquisition, Supervision, Methodology; **Qi Wang:** Methodology, Conceptualization, Software, Investigation; **Tao Su:** Methodology, Software, **Zhikai Zhao:** Methodology, Conceptualization.

References

Ahmadi-Baloutaki, M., Carriveau, R., & Ting, D. S. (2016). A wind tunnel study on the aerodynamic interaction of vertical axis wind turbines in array configurations. *Renewable Energy, 96*, 904-913. https://doi.org/10.1016/j.renene.2016.05.060

Bianchini, A., Balduzzi, F., Di Rosa, D., & Ferrara, G. (2019). On the use of Gurney Flaps for the aerodynamic performance augmentation of Darrieus wind turbines. *Energy Conversion and Management, 184*, 402-415. https://doi.org/10.1016/j.enconman.2019.01.068

Chehouri, A., Younes, R., Ilinca, A., & Perron, J. (2015). Review of performance optimization techniques applied to wind turbines. *Applied Energy, 142*, 361-388. https://doi.org/10.1016/j.apenergy.2014.12.043

Chen, C., Hu, E., Xu, Z., Tian, S. & Zhang, H. (2022). Design and analysis of a novel biomimetic folding fan two way variable automotive tail wing. *Mechanical Electrical Information*, (10), 37-

40. https://doi.org/10.19514/j.cnki.cn32-1628/tm.2022.10.010.

Ge, W., WU, D., Miao, D., & Wang, Y. (2022). Research on the influence of spoilers on the three-dimensional aerodynamic performance of wind turbine blades. *Solar Energy* (07),9 2-98. https://doi.org/10.19911/j.1003-0417.tyn20210510.01.

GWEC—Global Wind Energy Council. 2023. Available online: https://gwec.net/globalwindreport2023/

Hou, L., Zhu, J., Wang, Q., & Chang, X. (2023) Hydrodynamic characteristics of collaborative control disturbance rudder based on ship directionality. *Journal of Huazhong University of Science and Technology (Natural Science Edition)*. https://doi.org/10.13245/j.hust.240530.

Hu, Z., & Fu, L. (2023). Flight test study on the effect of large civil aircraft spoilers on the load of trailing edge flaps. *Machine Design and Manufacturing Engineering*, (11), 58-61. https://d.wanfangdata.com.cn/periodical/jxsjyzzgc202311012

Li, Y., Tong, G., Ma, Y., Feng, F., & Tagawa, K. (2023). Numerical study on aerodynamic performance improvement of the straight-bladed vertical axis wind turbine by using wind concentrators. *Renewable Energy*, *219*, 119545. https://doi.org/10.1016/j.renene.2023.119545

Rezaeiha, A., Montazeri, H., & Blocken, B. (2018). Towards accurate CFD simulations of vertical axis wind turbines at different tip speed ratios and solidities: Guidelines for azimuthal increment, domain size and convergence. *Energy Conversion and Management*, *156*, 301-316. https://doi.org/10.1016/j.enconman.2017.11.026

Shah, S. R., Kumar, R., Raahemifar, K., & Fung, A. S. (2018). Design, modeling and economic performance of a vertical axis wind turbine. *Energy Reports*, *4*, 619-623. https://doi.org/10.1016/j.egyr.2018.09.007

Subramanian, A., Yogesh, S. A., Sivanandan, H., Giri, A., Vasudevan, M., Mugundhan, V., & Velamati, R. K. (2017). Effect of airfoil and solidity on performance of small scale vertical axis wind turbine using three dimensional CFD model. *Energy*, *133*, 179-190. https://doi.org/10.1016/j.energy.2017.05.118

Wong, K. H., Chong, W. T., Poh, S. C., Shiah, Y. C., Sukiman, N. L., & Wang, C. T. (2018). 3D CFD simulation and parametric study of a flat plate deflector for vertical axis wind turbine. *Renewable Energy*, *129*, 32-55. https://doi.org/10.1016/j.renene.2018.05.085

Zhao, Z., Wang, D., Wang, T., Shen, W., Liu, H., & Chen, M. (2022). A review: Approaches for aerodynamic performance improvement of lift-type vertical axis wind turbine. *Sustainable Energy Technologies and Assessments*, *49*, 101789. https://doi.org/10.1016/j.seta.2021.101789

Zhu, X., Guo, Z., Zhang, Y., Song, X., Cai, C., Kamada, Y., & Maeda, T. (2022a). Numerical study of aerodynamic characteristics on a straight-bladed vertical axis wind turbine with bionic blades. *Energy*, *239*, 122453. https://doi.org/10.1016/j.energy.2021.122453

Zhu, X., Guo, Z., Zhang, Y., Song, X., Cai, C., Kamada, Y., & Maeda, T. (2022b). Numerical study of aerodynamic characteristics on a straight-bladed vertical axis wind turbine with bionic blades. *Energy*, *239*, 122453. https://doi.org/10.1016/j.energy.2021.122453